Lasers in Medical Science (2019) 34:1627–1635
https://doi.org/10.1007/s10103-019-02759-8

ORIGINAL ARTICLE

Evaluation of nonlinear optical behavior of mouse colon cancer cell line CT26 in hyperthermia treatment

Alireza Ghader[1] · Arezoo Mohammadi Gazestani[2] · Soraya Emamgholizadeh Minaei[3] · Ali Abbasian Ardakani[4] · Samideh Khoei[2] · Salman Mohajer[1] · Mohammad Hosein Majles Ara[1]

Received: 3 January 2019 / Accepted: 22 February 2019 / Published online: 11 March 2019

Abstract

Hyperthermia treatment can induce component changes on cell. This study explored the potential of Z-scan to improve accuracy in the identification of subtle differences in mouse colon cancer cell line CT26 during hyperthermia treatment. Twenty-one samples were subjected individually to treatment of hyperthermia at 41, 43, and 45 °C. Each hyperthermia treatment was done in six different time (15, 30, 45, 60, 75, and 90 min). Two optical setups were used to investigate the linear and nonlinear optical behavior of samples. Prior to the Z-scan technique, all samples were fixed with 1 mL of 5% paraformaldehyde. The linear optical setup indicated that extinction coefficient cannot monitor cell changes at different treatment regimes. But the nonlinear behavior of CT26 in all hyperthermia treatment regimens was different. By increasing the time and/or temperature of hyperthermia treatments, change in the sign of nonlinear refractive index from negative to positive occurred in earlier time intervals. This phenomenon was seen for 41, 43, and 45 °C in 75, 60, and 45 min, respectively. The results showed that the Z-scan technique is a reliable method with the potential to characterize cell changes during hyperthermia treatment regimes. Nonlinear refractive index can be used as a new index for evaluation of cell damage.

Keywords Colon cancer · Hyperthermia · Nonlinear refractive index · Z-scan technique

Introduction

Cancer is a major public health challenge worldwide, while colon cancer has been estimated to cause 8% of death in the USA [1]. For cancer therapy, several approaches are applied such as radiotherapy, surgery, and chemotherapy and in spite of their limitations, are considered the main conventional methods in cancer treatment [2]. Recently in many studies, hyperthermia is chiefly used as an adjuvant therapy and not as a sole one [3–5].

Hyperthermia is identified as an artificial procedure of increasing temperature from 41 to 45 °C by external sources [6]. The effects of hyperthermia in cells are dependent on exposure time and temperature. These effects, among others, are protein denaturation, induction of the apoptotic cascade, changes in cell-cycle regulatory signaling pathways, and DNA damage directly [7, 8].

Apoptosis ("programmed cell death") is a widespread biological process and is responsible for deletion of cells in normal tissues. It occurs normally during aging and development as a homeostatic mechanism to retain cell populations in tissues [9]. The main effect of hyperthermia is on proteins including denaturation, unfolding, and aggregation with other proteins. By this, myriads of activities in the cell occur that can lead to cell death. Hyperthermia at a temperature below 41 °C results in the expression of heat shock proteins that can cause thermotolerance but mild hyperthermia (41–45 °C) leads to the expression of the proinflammatory cytokine genes that may induce apoptosis [10]. Moreover, damage to DNA is

✉ Ali Abbasian Ardakani
A.ardekani@live.com

✉ Samideh Khoei
khoei.s@iums.ac.ir; skhoei@gmail.com

[1] Biophotonics Lab, Applied Science Research Center (ASRC), Kharazmi University, Karaj, Iran

[2] Department of Medical Physics, School of Medicine, Iran University of Medical Sciences, Tehran, Iran

[3] Department of Medical Physics and Imaging, Urmia University of Medical Sciences|, Urmia, Iran

[4] Department of Radiology Technology, School of Allied Medical Sciences, Shahid Beheshti University of Medical Sciences, Tehran, Iran

another effect of hyperthermia. Heat induction causes numerous impairments in DNA repair pathways. To these ends, the accumulation of DNA lesions leads to cell death [11].

There are several methods to determine the cytogenetic and cytotoxicity effects of different therapies and hyperthermia, such as real-time PCR, agarose gel electrophoresis, metaphase analysis, MTT, colony, and comet assays [12–16]. In recent years, biomedical studies have been developed to assist medical sciences in diagnosis processes [17–19]. Z-scan is an optical method that characterizes nonlinear optical properties. It was first described in 1990 by Sheik-Bahae et al. [20]. In this method, nonlinear refractive index is measured by steering the laser beam in defined distance around the focal zone. The coherent light affects medical diagnostic methods by improving the precise and decreasing the time of the process. These methods are not invasive generally. However, the Z-scan method has been used in estimation of biomarker concentration in blood serums [21, 22] and differentiation of tissue type [23, 24].

As earlier mentioned, hyperthermia treatment can induce component changes on the cell. The aim of this study was to evaluate Z-scan technique in monitoring cell changes on hyperthermia treatment at different temperatures and time exposure. To the best of our knowledge, this is the first study that used Z-scan to monitor cell changes at different treatment regimes.

Materials and methods

Materials

Cell culture reagents including Roswell Park Memorial Institute (RPMI) 1640, Fetal Bovine Serum (FBS), penicillin, and streptomycin were purchased from Gibco (Invitrogen, USA). Paraformaldehyde solution, EDTA, trypsin, and crystal violet were obtained from Sigma chemical company (St. Louis, MO, USA). Incubator (Memmert, Germany) and water bath hyperthermia (Memmert, Germany) were used for cellular experiments.

Cell culture

The mouse colon cancer cell line CT26 was obtained from Pasteur Institute of Iran. Cells were cultured in RPMI 1640 supplemented with 10% fetal bovine serum (FBS), penicillin (100 units/mL), and streptomycin (100 mg/mL) in 5% CO_2 and 95% air at 37 °C in a humidified incubator. Cells were harvested by trypsinizing cultures with 1 mm EDTA/0.25% trypsin (w/v) in PBS. Cells were trypsinized from the original flask and seeded in a number of 6×10^4 in 35 mm cell culture dish with one sterilized glass slide (lamella) at its bottom. Also, 2 ml culture media was added to each dish then plates were moved to an incubator for 48 h. Thereafter, plates were placed in water bath at temperatures of 41, 43, and 45 °C with different time durations (15, 30, 45, 60, 75, and 90 min). Immediately, samples were fixed with 1 mL of 5% paraformaldehyde and were prepared for Z-scan studies. Each procedure was repeated three times. In addition, one sample without treatment was obtained as a standard reference for further analysis and comparisons. Hence, 57 samples were prepared in this study. Finally, optical microscope images were obtained for all samples with a phase contrast inverted microscope (BEL, Monza, Italy).

Optical method

Two optical setups were used to investigate the linear and nonlinear optical behavior of samples. In this study, QG-532 Nd:YAG Q-switched laser (Crystal Laser, USA) operating at 532 nm wavelength were used. Also, 11XLP12-3S-H2 extreme low-power laser detector (Standa, Lithuania) was used to detect laser beam after interaction with sample.

Linear optical setup

Laser, polarizer (30-mm diameter, OptoSigma, Japan), and detector were utilized to determine the linear behavior of samples (Fig. 1a). Transmitted power was traced by changing the input of laser. Input and transmitted power (P_0 and P) were measured to compute extinction coefficient (EC) of each sample [25]. The slope of linear fit of output power versus input power was obtained as "m." Therefore, EC can be calculated as follows:

$$EC = (1/L) \times (Ln(1/m)) \quad (1)$$

where L is the thickness of the sample.

Nonlinear optical setup

The sign of nonlinear refraction can be investigated by using the closed aperture Z-scan method (Fig. 1b). By this method, the value of the nonlinear refractive index can also be calculated. The laser beam is focused by a lens (Reasonable Plano Convex Lens BK7 with 80 mm focal length, OptoSigma, Japan). The focused beam moves along the Z-axis to reach the aperture. Sample is shifted along the Z-axis (from −Z to +Z in the vicinity of the focus in the same paces), contributing to change in the power of incident light. As the sample is moved along the Z-axis, the transmittance power through the aperture is measured via movement. As a result of the movement, the light intensity can be decreased or increased on the aperture plan.

The value of the nonlinear refraction can be computed according to Eq. 2 [20, 25].

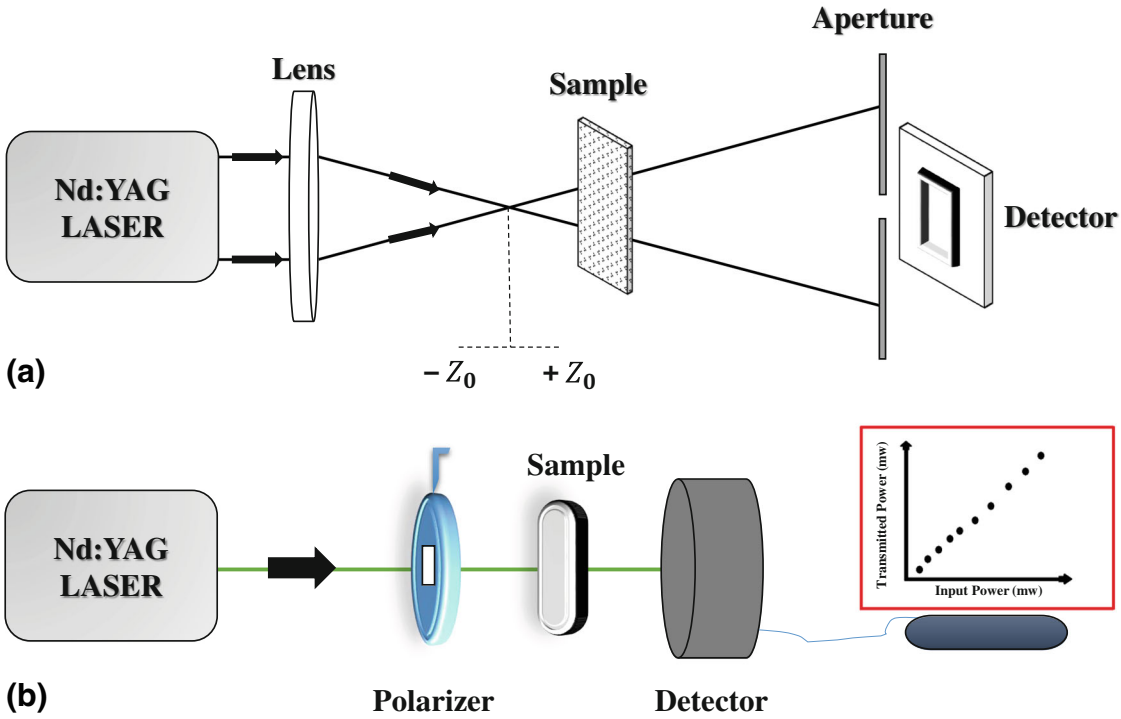

Fig. 1 Experimental setup for **a** extinction coefficient measurement and **b** Z-scan technique

$$n_2 = (\lambda\,\Delta T_{\mathrm{P-V}})/\left(2\pi\,L_{\mathrm{eff}}\,(0.406)\,(1-\mathrm{S})^{0.25}\,I_0\right) \quad (2)$$

where λ is the wavelength of the beam source. I_0 is the maximum intensity at the focus beam as follows:

$$I_0 = (2P)/\left(\pi\,(W_0)^2\right) \quad (3)$$

where W_0 and P are the beam waist and the input power, respectively. L_{eff} is effective length, which is calculated according to Eq. 4.

$$L_{eff} = \left(1-e^{-\alpha-L}\right)/\alpha \quad (4)$$

where α and L are the linear absorption coefficient and the thickness of the sample, respectively. In Eq. 2, S is linear transmittance of the aperture as following:

$$S = 1-\exp\left(-2(r_a/W_a)^{-2}\right) \quad (5)$$

where r_a is the radius of aperture and W_a is the radius of beam on the aperture plane.

$\Delta T_{\mathrm{P\text{-}V}}$ can be defined the difference between the highest and the lowest points in the graph of normalized transmittance (T_{P}-T_{V}). If there is a peak at first and valley afterward in the curve of normalized transmittance, the n_2 will be negative. Unlike that, if the peak comes after the valley, the n_2 will be positive.

Evaluation of the cytotoxic effects of hyperthermia treatment using clonogenic assay

Clonogenic assay was used to evaluate the overall toxicity of different hyperthermia treatment regimens. The CT26 cell line at a density of 6×10^4 was cultured in 35 mm cell culture dish for 24 h. After 24 h, the dishes were placed in water bath at temperatures of 41, 43, and 45 °C with different time durations (15, 30, 45, 60, 75, and 90 min). Then, the treated and control cells were harvested and single cell suspensions were seeded in 5 ml RPMI-1640 supplemented with 10% FBS in 60 mm Petri dishes. The cells were incubated at 37 °C in a humidified atmosphere of 5% CO_2. After 5 days, the colonies were fixed using 5% paraformaldehyde, stained with 0.5% crystal violet, and counted by an inverted phase microscope (MoticAE30). Finally, the plating efficiency (PE) and surviving fraction (SF) were calculated by the following equation, respectively:

$$PE\,(\%) = (Number\ \ of\ \ colonies\ \ counted/Number\ \ of\ \ cells\ \ seeded) \times 100 \quad (6)$$

$$Surviving\ fraction\ (SF) = (Colonies\ counted)/(Cells\ seeded \times (PE/100)) \quad (7)$$

Results

The SF of all hyperthermia treatment regimens were compared with results of this study to confirm the proposed optical methods (Table 1). Figure 2 shows the phase contrast microscope images of mouse colon cancer cell line CT26 on

Table 1 Effects of different hyperthermia treatment regimens (41, 43, and 45 °C) in different times (0, 15, 30, 45, 60, 75, and 90 min) on colony formation ability

Time (min)	SF of different hyperthermia treatment		
	41 °C	43 °C	45 °C
0	1.00	1.00	1.00
15	0.937	0.932	0.82
30	0.9	0.895	0.64
45	0.885	0.72	0.52
60	0.844	0.62	0.38
75	0.797	0.5	0.25
90	0.777	0.39	0.15

different treatment regimes. By increasing the temperature and heating time, cell membrane destroyed and the viability decreased (Table 1 and Fig. 2).

Linear optical behavior of samples

Input and transmitted power were utilized to calculate EC of samples. The EC of samples are presented in details in Table 2 and Fig. 3. The control samples and 15-min hyperthermia at 41 °C and 43 °C have the maximum amounts of EC (70.52 1/cm). It was observed that by increasing the time in all three temperatures, the amount of EC was decreased. Also 75- and 90-min hyperthermia at 45 °C had minimum of EC (22.77 1/cm). In addition, by increasing time from 60- to 70-min hyperthermia at 41 °C, the EC was significantly decreased (62.25 1/cm to 25.39 1/cm). Furthermore, this significant decrease occurred at 43 °C (45 to 60 min) and 45 °C (30 to 45 min).

Nonlinear optical behavior of samples

Curves of the normalized transmittance versus Z-axis are plotted for the samples prepared with various temperatures in different time durations. Figure 4 shows nonlinear optical behavior of samples for temperatures of 41, 43, and 45 °C. The control samples have the maximum amounts of $\Delta T_{P\text{-}V}$ among the samples with negative nonlinear refractive index for temperatures of 41, 43, and 45 °C and $\Delta T_{P\text{-}V}$ of these samples declined by increase in time. However, the minimum amounts of $\Delta T_{P\text{-}V}$ between samples with negative nonlinear refractive index are 60, 45, and 30 min for temperatures of 41, 43, and 45 °C respectively. In addition, the maximum of $\Delta T_{P\text{-}V}$ among the samples with positive nonlinear refractive index for temperatures of 41, 43, and 45 °C is 75, 60, and 45 min, respectively and $\Delta T_{P\text{-}V}$ of these samples decreased by increasing time. Also, the samples of 90 min have the smallest values of $\Delta T_{P\text{-}V}$ between the samples with positive nonlinear refractive index for these temperatures.

The Z-scan test was performed for all samples at temperatures of 41, 43, and 45 °C. The nonlinear refractive index of the control samples measured in all temperatures was negative. For the samples heated at 41 °C, the reported nonlinear refractive index was negative at 15, 30, 45, and 60 min, and its magnitude was decreased by increasing the heating time. But the sign of nonlinear refractive index changed into positive

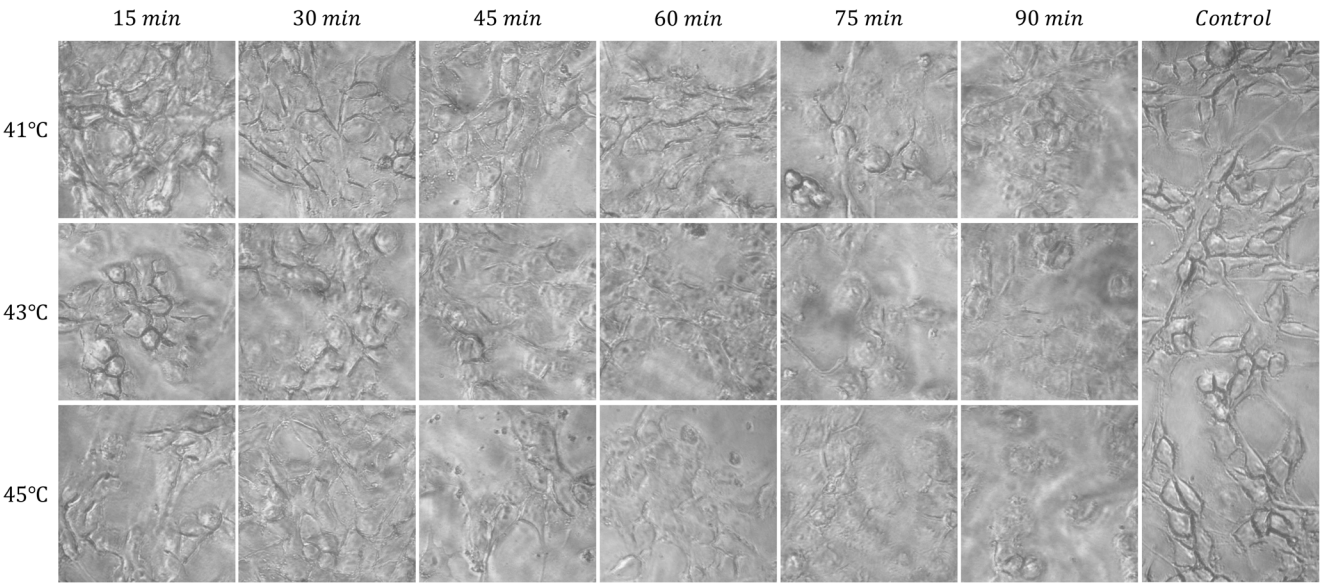

Fig. 2 Sample of phase contrast microscope images of colon cancer cell line on different hyperthermia treatment regimes. All of the microscope images were obtained with × 400 magnification

Table 2 Values of extinction coefficient for all samples

Samples	Extinction coefficient (1/cm)		
	41 °C	43 °C	45 °C
Control	70.52 ± 4.23	70.52 ± 4.23	70.52 ± 4.23
15 min	70.52 ± 4.23	70.52 ± 4.23	66.29 ± 3.98
30 min	66.29 ± 3.98	62.25 ± 3.73	66.29 ± 3.98
45 min	66.29 ± 3.98	58.38 ± 3.50	29.43 ± 1.77
60 min	62.25 ± 3.73	29.43 ± 1.77	25.39 ± 1.52
75 min	25.39 ± 1.52	28.07 ± 1.68	22.77 ± 1.37
90 min	24.08 ± 1.44	28.07 ± 1.68	22.77 ± 1.37

after 75 and 90 min. The behavior of nonlinear refractive index in the two other temperatures was similar to those of samples heated at 41 °C but change in sign occurred at different times for each temperature. For instance, the sign of nonlinear refractive index of samples heated at 43 °C changed after 60 min and became positive. Whereas, for the samples heated at temperature of 45 °C, the change occurred after 45 min. Moreover, it can be seen that positive values of the refractive index decreased by increase of the temperature. The results are presented in details according to Table 3. Also, calculated values of nonlinear refractive index of all samples are illustrated as a bar chart in Fig. 5.

Discussion

In this study, two different optical methods were used to evaluate optical behavior of mouse colon cancer cell line CT26 in hyperthermia treatment. The linear optical setup indicated that EC cannot monitor cell changes at different treatment regimes. In this regard, EC between control and 15-min and between 30- and 45-min hyperthermia at 41 °C, between control and 15-min and between 75- and 90-min hyperthermia at 43 °C, between 15- and 30-min and between 75- and 90-min hyperthermia at 45 °C were similar (Table 2 and Fig. 3). But the nonlinear behavior of CT26 in all hyperthermia treatment regimens was different (Table 3 and Fig. 5).

As shown in Fig. 5, the results indicated that by increasing the heating time, the sign of nonlinear refractive index changed into positive and this behavior was similar in each temperature. Whereas, the only difference between the samples is the time of change in sign. Previous studies have reported that hyperthermia therapy may weaken or kill tumor cells. The results confirmed that elevation of heating can lead to the production of DNA breaks after exposing Chinese hamster ovary cells to 45 °C. Moreover, the results showed that a reduction in the size of DNA occurs after an acute heat shock at 45 °C [26]. Survival fraction of Chinese hamster lung cells in hyperthermia treatment from 41.5 to 45.5 °C was analyzed by Laszlo et al. with gel electrophoresis assay. Their results

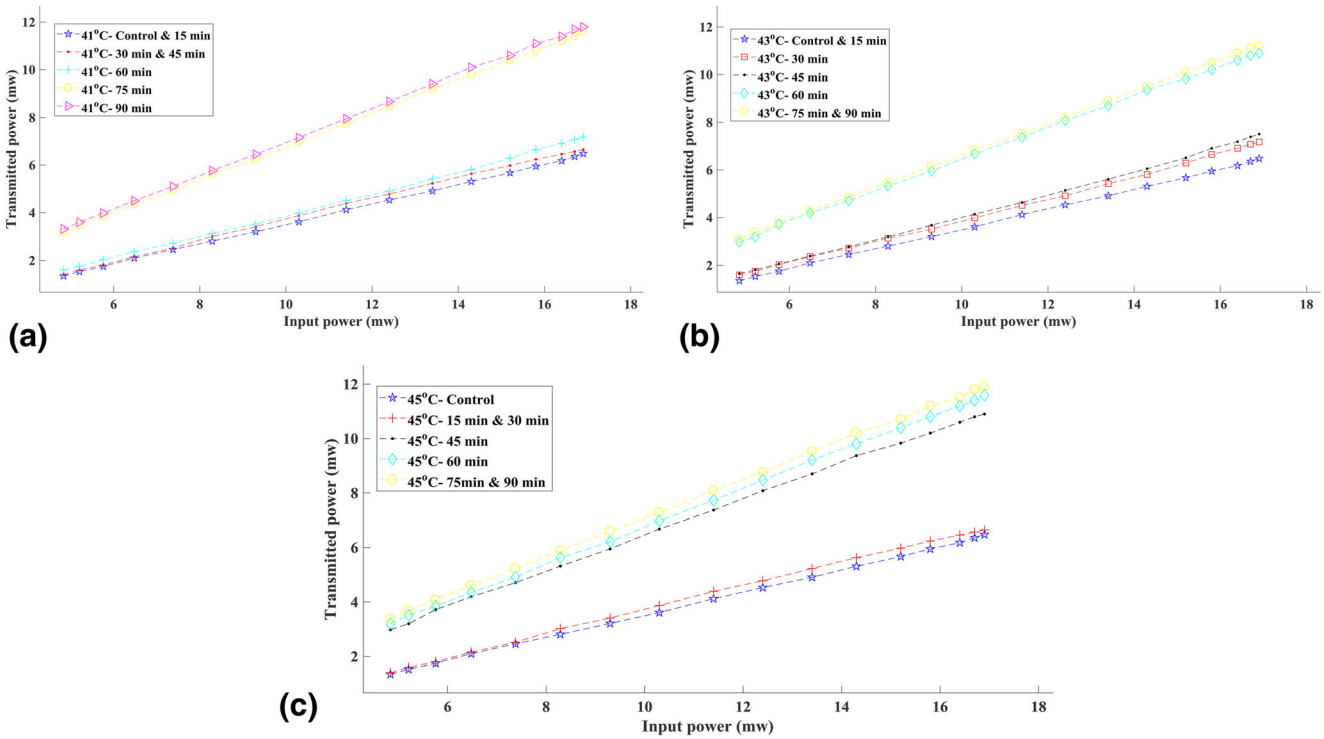

Fig. 3 Transmitted versus input power chart for calculate extinction coefficient of samples: **a** 41 °C; **b** 43 °C; **c** 45 °C

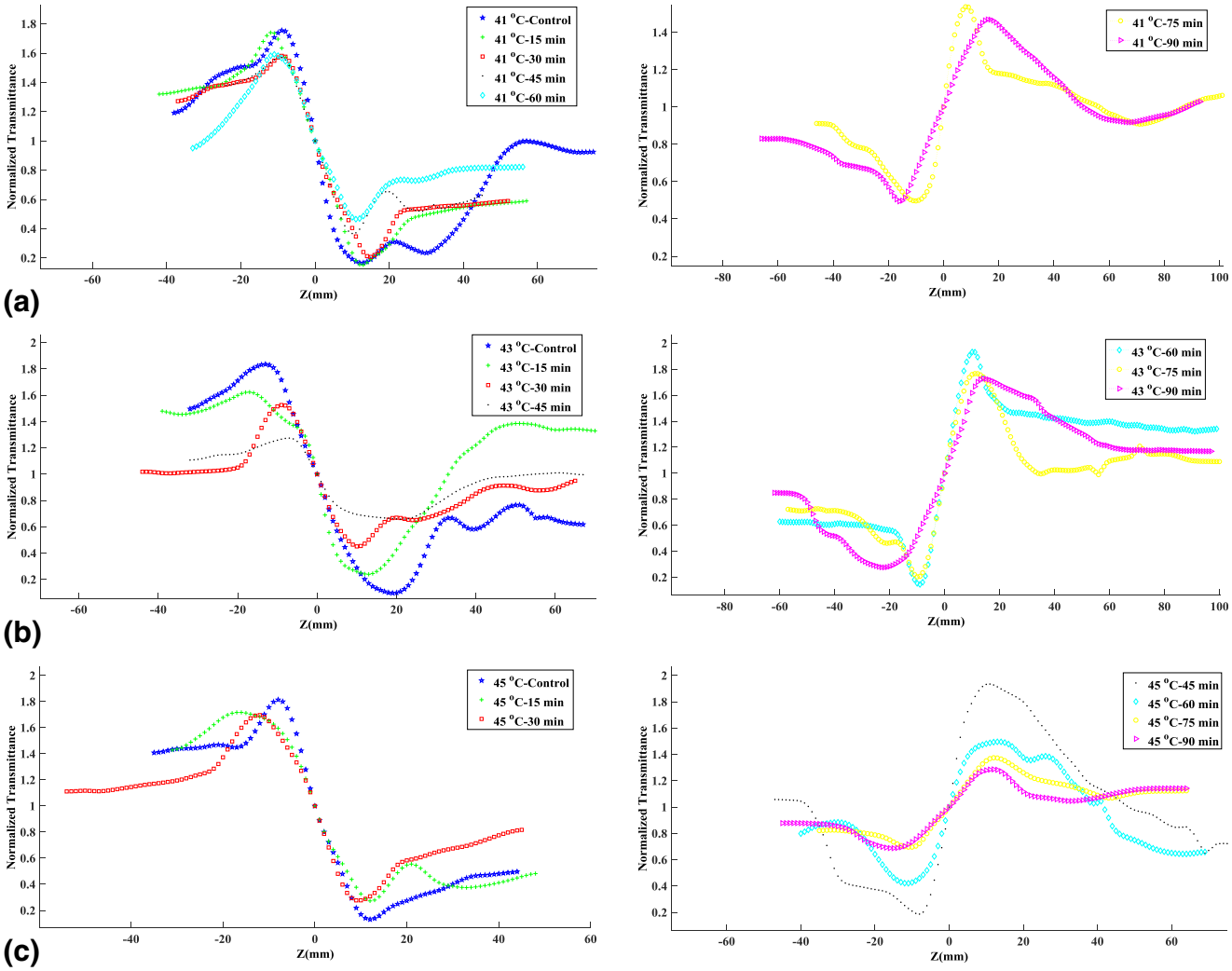

Fig. 4 Closed aperture Z-scan normalized data for different hyperthermia regimes and temperatures: **a** 41 °C; **b** 43 °C; and **c** 45 °C. Samples with negative and positive nonrefractive index were located in left and right of figure respectively

revealed that as temperature increased to 45.5 °C, survival of cells decreases [27]. Anai et al. have demonstrated that heat treatment of HeLa cells at 43 °C within 15 min led to the induction of DNA strand breaks. However, the increase of exposure time to 120 min has caused many double-strand breaks [28]. Sellins et al. showed that temperature elevation of murine thymocyte cell line to 43 °C in water bath induces apoptosis cell death and in this study was used to evaluate the effect of hyperthermia [29]. In addition, Takano et al. have studied apoptosis produced by 43 °C heating. Their findings showed that cell death was induced by 43 °C heating for 30 min in murine mastocytoma and in two human Burkitt's lymphoma lines, which was demonstrated by agarose gel electrophoresis [30]. Additionally, Yonwzawa et al. investigated the effect of hyperthermia on malignant fibrous histiocytoma cell line by agarose gel electrophoresis. In their studies, cells were subjected to hyperthermic stress at 41–44 °C for 1 h, and the cells undergo apoptosis when exposed to heat shock at 42–43 °C [31].

Table 3 Values of nonlinear refractive index for all samples

Samples	Nonlinear refractive index ($n_2 \times 10^{-6}$ cm^2/w ± error)		
	41 °C	43 °C	45 °C
Control	− 17.68 ± 1.06	− 17.15 ± 1.03	− 18.11 ± 1.09
15 min	− 15.66 ± 0.94	− 14.49 ± 0.87	− 16.62 ± 1.00
30 min	− 14.17 ± 0.85	− 10.57 ± 0.63	− 14.88 ± 0.89
45 min	− 13.21 ± 0.79	− 7.38 ± 0.44	+ 25.14 ± 1.51
60 min	− 10.91 ± 0.65	+ 24.57 ± 1.47	+ 14.77 ± 0.89
75 min	+ 14.63 ± 0.88	+ 20.59 ± 1.23	+ 8.95 ± 0.54
90 min	+ 11.08 ± 0.66	+ 20.31 ± 1.22	+ 7.38 ± 0.44

In the present study, the results showed that by increasing temperature from 41 to 45 °C, change in the sign of nonlinear refractive index occurs at less time intervals (75, 60, and

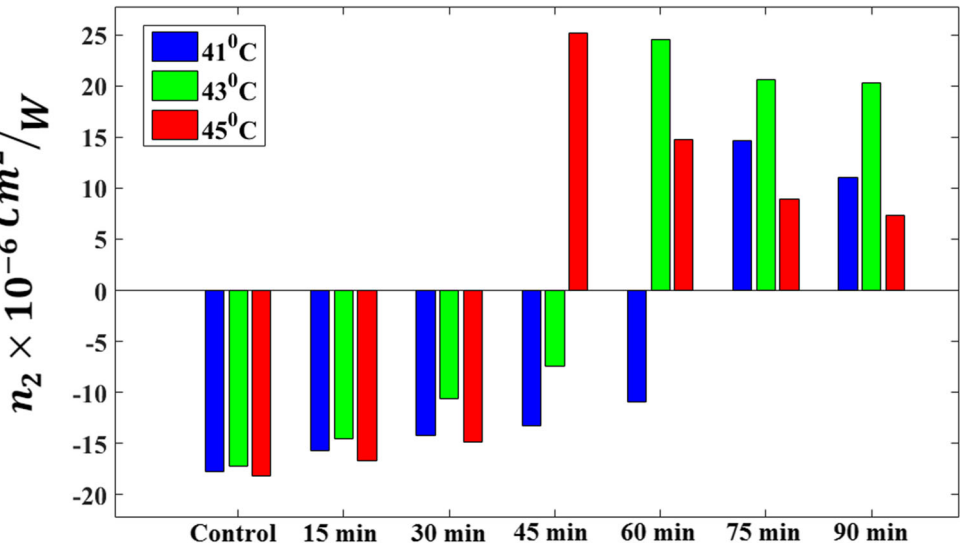

Fig. 5 Values of nonlinear refractive index of all samples

45 min for 41, 43, and 45 °C, respectively). This finding is completely in line with previous studies. By increasing temperature, cell death occurs at shorter time intervals. Therefore, change in the sign of refractive index can be used as an indicator of cell death. There are a number of possible explanations for these phenomena. In the present study, we can correlate the values of nonlinear refractive index with the aspects of the effect of hyperthermia on colon cancer cells: (1) protein denaturation, (2) apoptotic death, (3) change in cellular structures, and (4) DNA damages. In this regard, light scattering in cell samples is affected by two phases of "micro-scattering" and "nano-scattering." Part of the light due to contact with macro-scale scattering diffusion and the other part are scattered through touch with nano-scale scattering in the environment [32–34]. The size of the cell and its nucleus are in the order of micrometer, also the components of nucleus and cell cytoplasm are in the order of nanometer [35]. Since the wavelength of the incident beam in the cell here is 532 nm, two-phase scattering of scattering particles that are larger and smaller than wavelength exist. These two phase scatterings can affect the total amount of sample cell scattering and change their scattering [36]. Therefore, when the cell is decomposed, components that are much smaller than wavelengths are added to the cellular environment, and the contribution of the phase of "nano-scattering" increases in total scattering. Therefore, cell decomposition is the main factor in changing the pattern of diffraction and consequently, the gradient of the graph from negative to positive. The change in the pattern of diffraction is due to the interaction of the incident beam with the distribution of the new electron charge, which occurred due to the destruction of the cell membrane [37]. Under the influence of this important change, the refractive index of the cell's environment also varies, and the specimen acts like a convex lens that is called self-focusing. The result of this behavior in the diagram is obtaining normalized power when sample approaches the focus which is increased by getting away from the focus.

In recent years, some efforts have been made to investigate the capability of Z-scan technique to diagnose cancer in the human brain [23], skin [38], and oral tissue [39]. These studies indicate promising results for identifying differences between cancerous and non-cancerous human tissue. In addition, the proposed method can be used in vitro to find differences between the two types of breast cancer [17]. The present study provided additional information about the relationship between nonlinear refractive index and cell damage. In this study, we focused on Z-scan ability to identify cell changes during different hyperthermia treatment regimes. The clonogenic results had shown that by increasing temperature and time, survival fraction decreased. Which these findings were in line with results of the Z-scan technique.

To identify any confounding factors, all optical properties of materials were tested individually. Since none of the materials have any nonlinear properties, these parameters were not determined as confounding factors in nonlinear optical study. In additions, after treatment, the culture media was removed and the cells on the glass slide were fixed with 4% paraformaldehyde solution for 20 min. Then to remove any fixative solution, all samples were washed with distilled water and dried. Hence, there was not any solution covering the samples. But the lamella had an optical absorption. Hence all absorption values were subtracted from final EC measurements. In the term of cell confluency, the optical measurements were done under the guide of a microscope and find the area with the same confluency to minimize variations.

There are several methods to determine the effect of hyperthermia and other therapies on cells in experiments, such as MTT, and colony assay, which have limitations including time-consuming and high cost. Our results indicate that Z-scan is a useful technique for monitoring cell changes during

hyperthermia treatment. It is a simple, rapid, and accurate technique and also does not have any cost like cytogenetic examinations.

Conclusions

In conclusion, a proposed bio-optical method seems useful for evaluation of cell after hyperthermia treatment in vitro. Preliminary results show that only nonlinear refractive index of cell is a useful end point and can be used as an auxiliary technique with cytogenetic examinations to characterize cells after hyperthermia treatment.

Compliance with ethical standards

Conflict of interest The authors declare that they have no conflict of interest.

Publisher's note Springer Nature remains neutral with regard to jurisdictional claims in published maps and institutional affiliations.

References

1. Siegel RL, Miller KD, Jemal A (2016) Cancer statistics, 2016. CA Cancer J Clin 66:7–30. https://doi.org/10.3322/caac.21332
2. Beik J, Abed Z, Ghoreishi FS, Hosseini-Nami S, Mehrzadi S, Shakeri-Zadeh A, Kamrava SK (2016) Nanotechnology in hyperthermia cancer therapy: from fundamental principles to advanced applications. J Control Release 235:205–221. https://doi.org/10.1016/j.jconrel.2016.05.062
3. Wust P, Hildebrandt B, Sreenivasa G, Rau B, Gellermann J, Riess H, Felix R, Schlag P (2002) Hyperthermia in combined treatment of cancer. Lancet Oncol 3:487–497. https://doi.org/10.1016/S1470-2045(02)00818-5
4. Horsman MR, Overgaard J (2007) Hyperthermia: a potent enhancer of radiotherapy. Clin Oncol 19:418–426. https://doi.org/10.1016/j.clon.2007.03.015
5. Kim J, Hahn E, Tokita N (1978) Combination hyperthermia and radiation therapy for cutaneous malignant melanoma. Cancer 41:2143–2148. https://doi.org/10.1002/1097-0142(197806)41:6%3C2143::AID-CNCR2820410610%3E3.0.CO;2-9
6. Rao W, Deng Z, Liu J (2009) A review of hyperthermia combined with radiotherapy/chemotherapy on malignant tumors. Crit Rev Biomed Eng 38:101–116. https://doi.org/10.1615/CritRevBiomedEng.v38.i1.80
7. Hehr T, Wust P, Bamberg M, Budach W (2003) Current and potential role of thermoradiotherapy for solid tumours. Oncol Res Treat 26:295–302. https://doi.org/10.1159/000071628
8. Baronzio GF, Hager ED (2008) Hyperthermia in cancer treatment: a primer. Springer Science & Business Media
9. Kerr JF, Winterford CM, Harmon BV (1994) Apoptosis. Its significance in cancer and cancer therapy. Cancer 73:2013–2026. https://doi.org/10.1002/1097-0142(19940415)73:8%3C2013::AID-CNCR2820730802%3E3.0.CO;2-J
10. Roti Roti JL (2008) Cellular responses to hyperthermia (40–46 C): cell killing and molecular events. Int J Hyperth 24:3–15. https://doi.org/10.1080/02656730701769841
11. Mantso T, Goussetis G, Franco R, Botaitis S, Pappa A, Panayiotidis M (2016) Effects of hyperthermia as a mitigation strategy in DNA damage-based cancer therapies. Semin Cancer Biol 37–38(Supplement C):96–105. https://doi.org/10.1016/j.semcancer.2016.03.004
12. Moussavi M, Haddad F, Matin M, Iranshahi M, Rassouli F (2018) Efficacy of hyperthermia in human colon adenocarcinoma cells is improved by auraptene. Biochem Cell Biol 96:32–37. https://doi.org/10.1139/bcb-2017-0146
13. van den Tempel N, Laffeber C, Odijk H, van Cappellen WA, van Rhoon GC, Franckena M, Kanaar R (2017) The effect of thermal dose on hyperthermia-mediated inhibition of DNA repair through homologous recombination. Oncotarget 8:44593–44604. https://doi.org/10.18632/oncotarget.17861
14. Gomaa IE, Gaber SAA, Bhatt S, Liehr T, Glei M, El-Tayeb TA, Abdel-Kader MH (2015) In vitro cytotoxicity and genotoxicity studies of gold nanoparticles-mediated photo-thermal therapy versus 5-fluorouracil. J Nanopart Res 2:1–11. https://doi.org/10.1007/s1105
15. Nemani KV, Ennis RC, Griswold KE, Gimi B (2015) Magnetic nanoparticle hyperthermia induced cytosine deaminase expression in microencapsulated E. coli for enzyme–prodrug therapy. J Biotechnol 203(Supplement C):32–40. https://doi.org/10.1016/j.jbiotec.2015.03.008
16. Nakagawa Y, Kajihara A, Takahashi A, Murata AS, Matsubayashi M, Ito SS, Ota I, Nakagawa T, Hasegawa M, Kirita T (2018) BRCA2 protects mammalian cells from heat shock. Int J Hyperth 34:795–801. https://doi.org/10.1080/02656736.2017.1370558
17. Ghader A, Ardakani AA, Ghaznavi H, Shakeri-Zadeh A, Minaei SE, Mohajer S, Ara MHM (2018) Evaluation of nonlinear optical differences between breast cancer cell lines SK-BR-3 and MCF-7; an in vitro study. Photodiagn Photodyn Ther 23:171–175. https://doi.org/10.1016/j.pdpdt.2018.06.015
18. Abbasian Ardakani A, Rajaee J, Khoei S (2017) Diagnosis of human prostate carcinoma cancer stem cells enriched from DU145 cell lines changes with microscopic texture analysis in radiation and hyperthermia treatment using run-length matrix. Int J Radiat Biol 93:1248–1256. https://doi.org/10.1080/09553002.2017.1359429
19. Park J, Hwang M, Choi B, Jeong H, Jung JH, Kim HK, Hong S, Park JH (2017) Exosome classification by pattern analysis of surface-enhanced Raman spectroscopy data for lung cancer diagnosis. Anal Chem 89:6695–6701. https://doi.org/10.1021/acs.analchem.7b00911
20. Sheik-Bahae M, Said AA, Wei T-H, Hagan DJ, Van Stryland EW (1990) Sensitive measurement of optical nonlinearities using a single beam. IEEE J Quantum Electron 26:760–769. https://doi.org/10.1109/3.53394
21. Ghader A, Majles Ara MH, Mohajer S, Divsalar A (2018) Investigation of nonlinear optical behavior of creatinine for measuring its concentration in blood plasma. Optik 158:231–236. https://doi.org/10.1016/j.ijleo.2017.12.063
22. de Queiroz Mello AP, Albattarni G, Espinosa DHG, Reis D, Neto AMF (2018) Structural and nonlinear optical characteristics of in vitro glycation of human low-density lipoprotein, as a function of time. Braz J Phys 48(6):560–570. https://doi.org/10.1007/s13538-018-0600-x
23. Hosseinzadeh M, Salmani S, Majles Ara M, Mohajer S (2018) The simple optical methods for early diagnosis of selected benign and malignant brain tumors of human. J of Nonlinear Optical Phys & Materials 27(03):1850033. https://doi.org/10.1142/S0218863518500339
24. Salman M, Hosein MAM, Mohammad N (2016) Nonlinear optical investigation of normal ovarian cells of animal and cancerous ovarian cells of human in-vitro. Optik 127:3867–3870. https://doi.org/10.1016/j.ijleo.2016.01.072

25. Mohajer S, Ara MHM, Serahatjoo L (2016) Effects of graphene quantum dots on linear and nonlinear optical behavior of malignant ovarian cells. J of Nanophotonics 10:036014. https://doi.org/10.1117/1.JNP.10.036014
26. Warters RL, Henle KJ (1982) DNA degradation in Chinese hamster ovary cells after exposure to hyperthermia. Cancer Res 42:4427–4432
27. Laszlo A (1988) Evidence for two states of thermotolerance in mammalian cells. Int Hyperth 4:513–526. https://doi.org/10.3109/02656738809027695
28. Anai H, Maehara Y, Sugimachi K (1988) In situ nick translation method reveals DNA strand scission in HeLa cells following heat treatment. Cancer Lett 40:33–38. https://doi.org/10.1016/0304-3835(88)90259-5
29. Sellins KS, Cohen JJ (1991) Hyperthermia induces apoptosis in thymocytes. Radiat Res 126:88–95. https://doi.org/10.2307/3578175
30. Takano YS, Harmon BV, Kerr JF (1991) Apoptosis induced by mild hyperthermia in human and murine tumour cell lines: a study using electron microscopy and DNA gel electrophoresis. J Pathol 163:329–336. https://doi.org/10.1002/path.1711630410
31. Yonezawa M, Otsuka T, Matsui N, Tsuji H, Kato KH, Moriyama A, Kato T (1996) Hyperthermia induces apoptosis in malignant fibrous histiocytoma cells in vitro. Int J Cancer 66:347–351. https://doi.org/10.1002/(SICI)1097-0215(19960503)66:3%3C347::AID-IJC14%3E3.0.CO;2-8
32. Cox A, DeWeerd AJ, Linden J (2002) An experiment to measure Mie and Rayleigh total scattering cross sections. Am J Phys 70:620–625. https://doi.org/10.1119/1.1466815
33. Tuchin VV (2007) Tissue optics: light scattering methods and instruments for medical diagnosis, vol 13. SPIE press, Bellingham
34. Maeda D, Iwai T, Namiki M (2018) Diffuse light reflectometry for measuring scattering and absorption coefficients of a biological tissue. In: Biomedical Imaging and Sensing Conference. Int Society for Optics and Photonics, p 107111L. https://doi.org/10.1117/12.2319355
35. Marshall WF, Young KD, Swaffer M, Wood E, Nurse P, Kimura A, Frankel J, Wallingford J, Walbot V, Qu X, Roeder AH (2012) What determines cell size? BMC Biol 10:101. https://doi.org/10.1186/1741-7007-10-101
36. Nishidate I, Mustari A, Kawauchi S, Sato S, Sato M, Kokubo Y (2017) In vivo imaging of tissue scattering parameter and cerebral hemodynamics in rat brain with a digital red-green-blue camera. SPIE BiOS Int Society for Opt and Photonics, 100500O-100508. https://doi.org/10.1117/12.2251109
37. Boyd RW (2008) Nonlinear opt. Academic Press
38. Behravan M, Salmani S, Kavianfar A, Gharibi A, Majles Ara M (2017) Early diagnosis by comparison between interferometry and Z-scan methods to measure NLO refraction of human skin cancer (BCC and SCC) in vitro. J Nonlinear Optical Phys Mater 26(03):1750033. https://doi.org/10.1142/S0218863517500333
39. Salman M, Hossein MAM, Kamran KS, Shayan M (2016) Optical discrimination of benign and malignant oral tissue using Z-scan technique. Photodiagn Photodyn Ther 16(Supplement C):54–59. https://doi.org/10.1016/j.pdpdt.2016.08.001